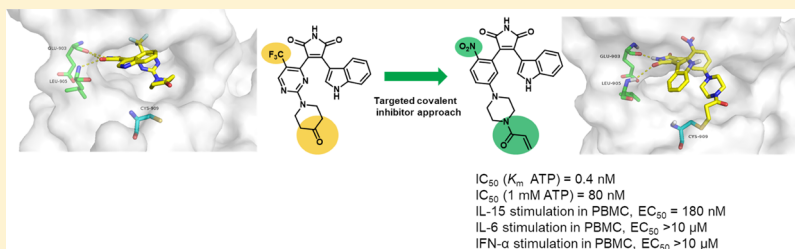


## Discovery of an Orally Available Janus Kinase 3 Selective Covalent Inhibitor

Liyang Shi, Zhenpeng Zhong, Xitao Li, Yiqing Zhou,<sup>1b</sup> and Zhengying Pan\*<sup>1b</sup>

State Key Laboratory of Chemical Oncogenomics, Engineering Laboratory for Chiral Drug Synthesis, Key Laboratory of Chemical Genomics, School of Chemical Biology and Biotechnology, Shenzhen Graduate School, Peking University, Shenzhen 518055, China

## Supporting Information



**ABSTRACT:** JAK family kinases are important mediators of immune cell signaling and Janus Kinase 3 (JAK3) has long been indicated as a potential target for autoimmune disorders. Intensive efforts to develop highly selective JAK3 inhibitors have been underway for many years. However, because of JAK3's strong binding preference to adenosine 5'-triphosphate (ATP), a number of inhibitors exhibit large gaps between enzymatic and cellular potency, which hampers efforts to dissect the roles of JAK3 in cellular settings. Using a targeted covalent inhibitor approach, we discovered compound **32**, which overcame ATP competition (1 mM) in the enzymatic assay, and demonstrated significantly improved inhibitory activity for JAK3-dependent signaling in mouse CTLL-2 and human peripheral blood mononuclear cells. Compound **32** also exhibited high selectivity within the JAK family and good pharmacokinetic properties. Thus, it may serve as a highly valuable tool molecule to study the overlapping roles of JAK family kinases in complex biological settings. Our study also suggested that for covalent kinase inhibitors, especially those targeting kinases with low *K<sub>m</sub>* ATP values, the reversible interactions between molecules and proteins should be carefully optimized to improve the overall potency.

## INTRODUCTION

Janus kinases (JAKs) and their downstream effectors, signal transducer and activator of transcription (STAT), are essential for T cell signal transduction. The JAK family has four members: JAK1, JAK2, JAK3, and TYK2. These members bind to cytokine receptors in pairs. JAK3 paired with JAK1 is involved in gamma common-chain cytokine signaling, including IL-2, IL-4, IL-7, IL-9, IL-15, and IL-21.<sup>1</sup> In contrast to other JAKs, which are broadly expressed, JAK3 is predominantly expressed in the hematopoietic system. It was initially assumed that specific inhibition of JAK3 could achieve selective and safe immunosuppressive effects.<sup>2</sup> However, tofacitinib (**1**, Figure 1A), the first approved drug targeting JAK3, is actually a pan-JAK inhibitor.<sup>3</sup> Novartis inhibitor NIBR3049 (**2**, Figure 1A), which is a potent JAK3 inhibitor with high selectivity within the JAK family, was significantly less potent in a cellular STAT5 phosphorylation assay compared with **1**, which suggested that specific inhibition of JAK3 alone was not sufficient to achieve immunosuppressive effects.<sup>4</sup> Presently, several selective JAK3 inhibitor programs have targeted covalent bond formation with Cys909 as an optimization strategy,<sup>5–12</sup> including PF-06651600 (**3**, Figure 1A) in clinical trials for inflammatory diseases. In this article, we present our efforts to develop covalent irreversible

inhibitors of JAK3 based on the same scaffold as **2**, and results from head-to-head comparisons in multiple assays suggest that specific inhibition of JAK3 alone is sufficient to interrupt JAK3-mediated signaling pathways. On the basis of these results, we suggest that the competition with high intracellular adenosine 5'-triphosphate (ATP) concentration may have resulted in the poor activity observed with compound **2**. We hypothesize that optimization of a scaffold, such as **2**, as a covalent inhibitor may ameliorate the poor cellular translation for selective JAK3 inhibitors. The initial attempt to develop covalent inhibitors failed to overcome the ATP competition. However, the results obtained indicated the importance of noncovalent interactions for developing highly effective covalent inhibitors.

Several reasons may be considered regarding the poor correlation between enzymatic and cellular activity for JAK3 inhibitors which include the use of the kinase domain alone to run the enzymatic assay, the relative contributions of JAK1 and JAK3 to the signaling pathway in cells, and the different *K<sub>m</sub>* ATP values among the JAK isoforms.<sup>13,14</sup> JAK3 kinase exhibits a significantly low *K<sub>m</sub>* ATP value,<sup>15</sup> indicating that the efficacy

Received: November 21, 2018

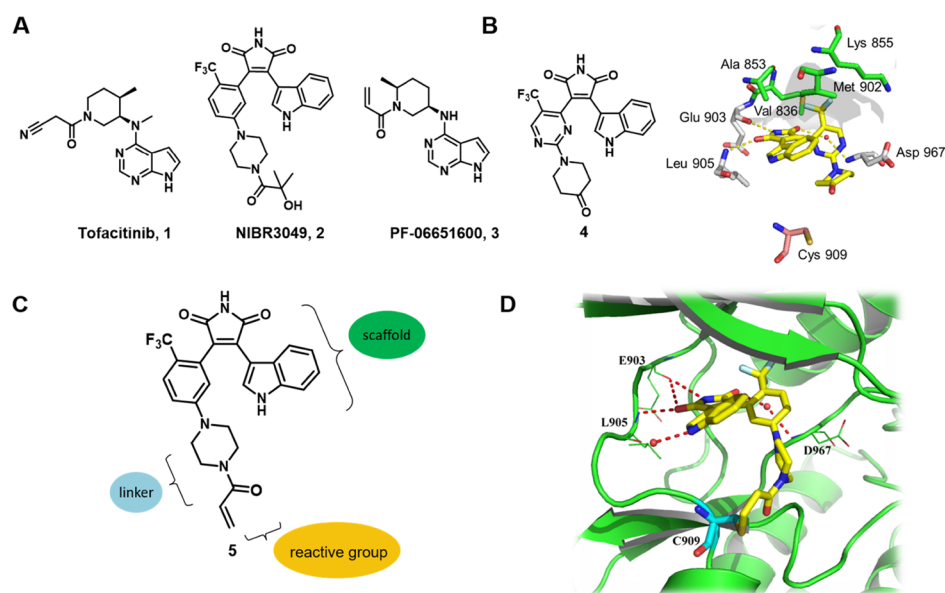


**Figure 1.** Design of covalent inhibitors of JAK3. (A) Chemical structures of tofacitinib (1), NIBR3049 (2), and PF-06651600 (3). (B) Chemical structure of compound 4 (left) and crystal structure (PDB code 3PJC) of compound 4 and JAK3.<sup>4</sup> (right) (C) Chemical structure of compound 5 and scaffold, linker, and reactive group regions. (D) Docking model of JAK3 (PDB code 3PJC) and compound 5. The red dashed lines indicate potential hydrogen bond interactions between JAK3 and compound 5.

of ATP-competitive JAK3 inhibitors could be significantly affected by the native substrate ATP concentration. If the high physiological ATP concentration is the main reason causing the loss of cellular potency of 2, then the cellular efficacy may be improved through a covalent inhibitor approach. Competition from intracellular ATP may be overcome by a selective, covalently bound JAK3 inhibitor, thus breaking the binding equilibrium of the native substrate and enzyme.<sup>16</sup>

## RESULTS AND DISCUSSION

**Design of Covalent Inhibitors.** A crystal structure of JAK3 and compound 4<sup>4</sup> (Figure 1B), a close analog of 2, was used as our design template. The maleimide ring forms two hydrogen bonds with the hinge region, and the piperidinone group points toward Cys909. Initial attempts involved maintaining essential hydrogen bonding interactions in the original scaffold and introducing a reactive group with a piperazine linker to yield compound 5 (Figure 1C,D). As expected, compound 5 exhibited a potent inhibition of JAK3 ( $IC_{50} = 1.5$  nM) (Table 1) with a potency similar to compound 2. However, compound 5 significantly lost its potency when the enzymatic assay was run in the presence of 1 mM ATP ( $IC_{50} = 520$  nM, Table 1).

**Compound 5 Covalently Binds to Cys909 and Irreversibly Inhibits JAK3.** Mass spectrometry was employed to examine whether a covalent bond was formed between compound 5 and JAK3. After incubation of the recombinant JAK3 kinase domain with compound 5, the complex was digested by trypsin and subjected to mass spectrometry. The mass peak of the Cys909-containing peptide fragment of recombinant JAK3 shifted from 1380 to 1874 Da (Figure S2). The increased molecular weight was equal to the molecular weight of compound 5. Further analysis of peak 1874 by MS/MS demonstrated that the modified site was indeed Cys909 (Figure S2). These results suggested that JAK3 and compound 5 formed a covalent adduct via Cys909.

**Table 1.** SAR of the Linker Region<sup>a</sup>

No.	R	$IC_{50}$ (nM)	
		$K_m$ (6 $\mu$ M) ATP	1 mM ATP
1	-	1.7	50
2	-	2.0	685
3	-	0.4	202
5		1.5	520
6		6.4	3456
7		41	ND
8		4.4	ND
9		21	>30000
10		21	3690
11		0.6	ND
12		0.6	1276
13		16	ND

<sup>a</sup>Compounds were measured at  $K_m$  ATP (6  $\mu$ M) and 1 mM ATP.  $IC_{50}$  values are reported as the means of duplicates. ND, not determined.

We also performed a time-dependent inhibition assay to independently determine whether compound 5 shared the

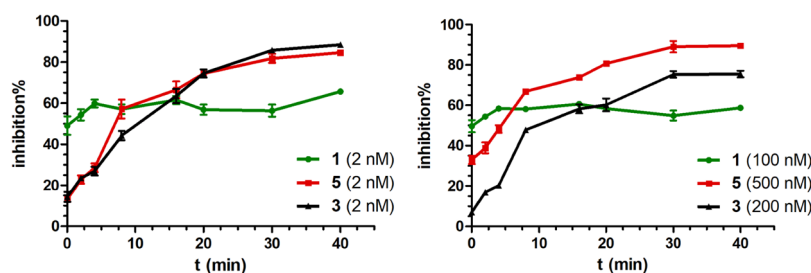


**Figure 2.** Time-dependent inhibition curves of compound **1**, **3**, and **5** at  $K_m$  (left) and 1 mM ATP (right).

features of irreversible inhibitors. Extending the preincubation time of compounds **3** and **5** with JAK3 improved the inhibitory effect both in the presence of  $K_m$  and 1 mM ATP (Figure 2), whereas the reversible inhibitor **1** did not exhibit such a time-dependent behavior.

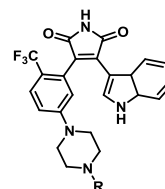
**Structure–Activity Relationship.** Although compound **5** was observed to be a covalent, irreversible inhibitor, a significant loss of potency was observed (JAK3  $IC_{50}$  = 520 nM) when the enzymatic assay was run in the presence of 1 mM ATP. It was clear that, in this case, merely forming a covalent bond between inhibitor and kinase was not sufficient to overcome the competition from endogenous ATP. Given that covalent inhibitors can be optimized by improving the reversible binding affinity and the inherent chemical reactivity of the electrophile,<sup>17</sup> we explored optimization opportunities from three directions: adjusting a suitable linker for better orientation of reactive groups, appending a more reactive warhead to increase chemical reactivity, and improving noncovalent binding interactions.

In hopes of better orienting toward Cys909, we attempted to adjust linker lengths and replace the piperazine with other cyclic rings or more flexible chains. Three to four atom spacing between the core scaffold and acrylamide group was preferred (**5**, **6**, **8**, **11**, **12** vs **7** and **13**, Table 1). Although variations in the flexible cyclic linkers did not afford appreciably more potent analogs (**6**, **8**, **9**, **10**, Table 1), the flexible chain linkers did exhibit a marginal improvement in JAK3 potency (**11** and **12**, Table 1). However, no improvement was observed with high ATP concentration for these analogs. Therefore, the piperazine moiety was retained as the preferred linker.

We then focused on tuning the reactivity of the warhead (Table 2). Switching the warhead from acrylamide to chloromethylketone or propynamide (**16** and **18**, Table 2) led to increased inhibitory activities, whereas introducing  $\beta$ -methyl or  $N,N$ -dimethylaminomethyl acrylamide decreased potency (**14** and **15**, Table 2). Bromomethylketone, a more reactive warhead, exhibited reduced inhibitory activity (**17**, Table 2), which may be because of its instability in the assay medium.

As optimization of the linker and reactive groups did not yield a compound with improved inhibitory activity of JAK3 at higher ATP concentrations, we focused on investigating the influence of noncovalent interactions around the core maleimide ring. On the basis of the crystal structure of JAK3 with compound **4** and our modeling studies (Figure 1B), we hypothesized that in addition to interactions with the hinge region, substitutions around the phenyl group and hydrophobic contacts between indole and side chains of Ala853 and Leu956 might be two regions to explore. Around the indole group, substituents did not have any substantial influence on the inhibitory effect (**19**–**23**, Table 3), but a significant

**Table 2.** SAR of Reactive Groups<sup>a</sup>



No.	R	$IC_{50}$ (nM)	
		$K_m$ (6 $\mu$ M) ATP	1 mM ATP
<b>14</b>		21	ND
<b>15</b>		104	ND
<b>16</b>		0.4	210
<b>17</b>		19	709
<b>18</b>		0.8	212

<sup>a</sup>Compounds were measured at  $K_m$  ATP (6  $\mu$ M) and 1 mM ATP.  $IC_{50}$  values are reported as the means of duplicates. ND, not determined.

reduction in potency occurred when indole was replaced with a phenyl group (**24**, Table 3), suggesting that a bulky indole group was preferred. By varying the substitutions on the phenyl group, we found that the preferred location of substitutions was at the position para- to the piperazine linkage, as meta- or ortho-decorations led to much weaker inhibitors (**25**–**26**, Table 3). No substitution on the phenyl group also resulted in a considerable loss in potency (**27**, Table 3), suggesting that occupancy in the pocket encompassed by the side chains of Val836, Ala853, Lys855, and Met902 was favorable for the potency. Therefore, we incorporated different substitutions at this para-position. Interestingly, we found that electron-withdrawing groups were more beneficial than electron-donating groups (**28**–**33**, Table 3). Compounds bearing strong electron-withdrawing nitro group can still preserve their potency reasonably well in the presence of high concentration of ATP (**31**–**33**, Table 3). However, replacing the phenyl group with an aliphatic chain resulted in a dramatic loss in potency (**34**, Table 3), indicating that the aromatic ring is an essential feature for retaining the potency. Noncovalent versions of compounds **5** and **32** were also tested for their inhibitory potencies (**35** and **36**, Table 3). Clearly, modification with a nitro group improved noncovalent interactions. On the basis of these results, we chose compound **32**, which harbors a nitro group and a mild acrylamide warhead, for further functional characterizations.

**Kinetics Characterization and Selectivity of Selected Compounds.** To better characterize contributions of

Table 3. SAR of the Scaffold<sup>a</sup>

NO.	R1	R2	IC <sub>50</sub> (nM)	
			K <sub>m</sub> (6 μM) ATP	1 mM ATP
5			1.5	520
19 <sup>b</sup>			2.0	584
20			2.8	817
21			5.4	895
22			7.5	650
23			4.0	750
24 <sup>b</sup>			4000	ND
25			894	ND
26			873	ND
27			232	ND
28			52	ND
29			21	ND
30			4.3	450
31			0.4	332
32			0.4	80
33			<0.1	90
34			1777	ND
35			27	1000
36			6	210

<sup>a</sup>Compounds were measured at K<sub>m</sub> ATP (6 μM) and 1 mM ATP. IC<sub>50</sub> values are reported as the means of duplicates. ND, not determined. <sup>b</sup>The synthetic routes of compounds were described in the Supporting Information.

reversible binding and covalent bond formation rate to our covalent inhibitors, we evaluated K<sub>i</sub> and k<sub>inact</sub> parameters of selected compounds (Table 4, Figure S3). Different para-substitutions on the phenyl group and linker variations exhibited greater impacts on binding affinity than reaction

Table 4. Kinetics Study<sup>a</sup>

compounds	K <sub>i</sub> (nM)	k <sub>inact</sub> (min <sup>-1</sup> )	k <sub>inact</sub> /K <sub>i</sub> (10 <sup>5</sup> M <sup>-1</sup> s <sup>-1</sup> )
5	1.0	0.21	35
32	1.1	0.41	62
6	27	0.21	1.3
10	201	0.26	0.22
11	9.4	0.25	4.4
18	55	1.2	3.6
29	51	0.17	0.56
30	3.3	0.07	3.5

<sup>a</sup>Kinetic parameters were measured with HTRF KinEASE assays. The starting concentration was dependent on IC<sub>50</sub> values of compounds, and concentrations from a threefold dilution series (six data points per curve) were applied. The collected data were fitted as described in the literature<sup>20</sup> to determine k<sub>inact</sub> and K<sub>i</sub>. GraphPad Prism was used for curved fitting.

rate. Compound 32 exhibited a very high binding affinity (K<sub>i</sub> = 1.1 nM) and a moderate inactivation rate (0.41 min<sup>-1</sup>) (Table 4). This feature of compound 32 may be beneficial to mitigate proteome-wide cross-reactivity and enhances its selectivity.

To investigate the selectivity, compound 32 was tested at 1 μM against a panel of 50 kinases and only found to potentially inhibit protein kinase C (PKCs) and glycogen synthase kinase 3-β (GSK3β) (>80% inhibition, both do not have a cysteine comparable to Cys909). This result was consistent with that of inhibitor 2.<sup>4</sup> Importantly, compound 32 also exhibited high selectivity within the JAK family and among other kinases with a cysteine at a comparable position to Cys909 (Figure 3), such as Bruton's tyrosine kinase, epidermal growth factor receptor, and interleukin-2-inducible T cell kinase.

**Compound 32 Selectively Inhibits JAK3-Dependent Signaling in Live Cells.** To test whether the nitro-group series of compounds was effective in a native cellular environment unlike its template compound 2, we evaluated its ability to inhibit STAT5 phosphorylation in live cells. After CTLL-2 cells were incubated with compound 32 for 2 h, IL-2-induced STAT5 phosphorylation was almost completely inhibited at a concentration of 0.6 μM (EC<sub>50</sub> = 305 nM; Figure 4A,B). In comparison, 6 μM was required in compound 2 treated cells to completely inhibit IL-2-induced STAT5 phosphorylation (EC<sub>50</sub> = 1999 nM, Figure 4A,B). To our surprise, compound 33, which harbors a more reactive warhead than 32, significantly lost its potency in this cellular assay, indicating that the cellular potency was not always proportional to the reactivity of warheads. Compound 32 was also more sensitive in inhibiting IL-15-induced STAT5 phosphorylation in CTLL-2 cells (EC<sub>50</sub> = 141 nM) (Figure 4B,C). Compared to compound 3, compound 32 exhibited comparable inhibitory activity in IL-15-stimulated STAT5 phosphorylation and slightly weaker potency in IL-2-induced STAT5 phosphorylation (Supporting Information, Figure S4). In human peripheral blood mononuclear cells (PBMCs) (Figure 4D), compound 32 was also more potent than compound 2 in both IL-2 and IL-15-induced STAT5 phosphorylation.

We further characterized the cellular selectivity of compound 32 in PBMCs upon stimulation with different cytokines (Figure 5). Among these cytokines, only signaling via IL-15 is dependent on JAK3. Signaling via IL-6 is dependent on JAK1/JAK2/TYK2, and signaling via IFN-α is exclusively mediated by JAK1/TYK2 signaling.<sup>1</sup> Compound 32 almost completely



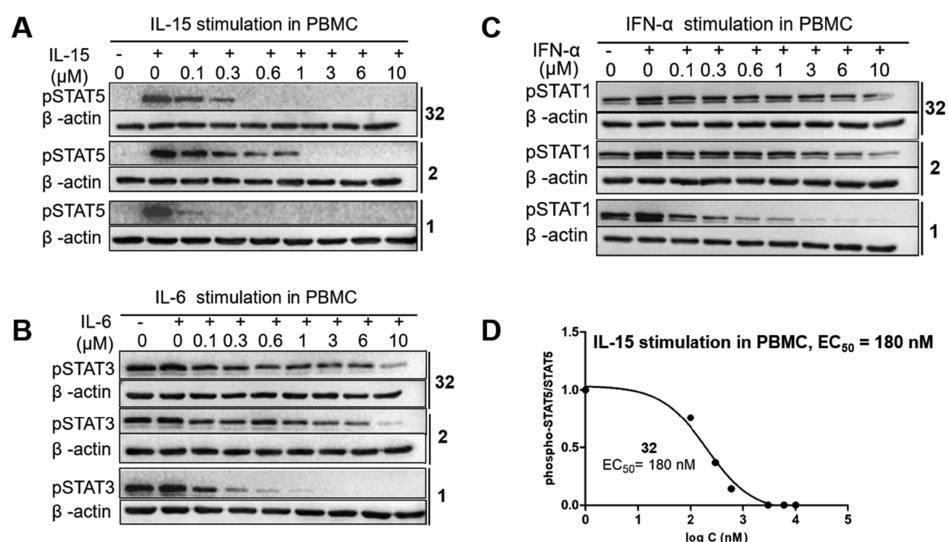


**Figure 5.** Compound 32 selectively inhibits JAK3-dependent cytokine signaling. PBMCs were preincubated with the indicated concentrations of compound 32, 2, and 1 for 2 h and stimulated for 30 min with IL-15 (A), IL-6 (B), and IFN- $\alpha$  (C). STAT5 (A), STAT3 (B), and STAT1 (C) phosphorylation was determined using specific phospho-antibodies and immunoblotting.  $\beta$ -actin levels were determined to demonstrate equal loading. Band intensities were quantified, and  $EC_{50}$  values were calculated using GraphPad Prism software (D).

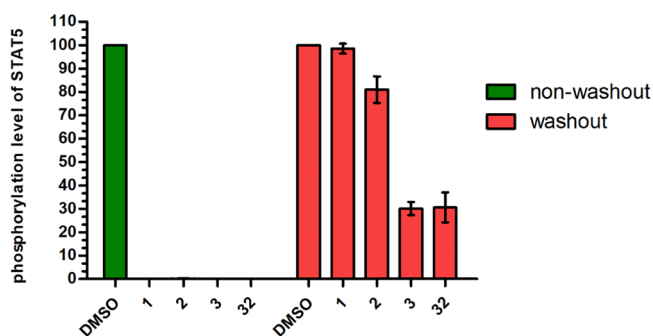


**Figure 6.** Compound 32 sustained inhibition of p-STAT5 after washout. CTLL-2 cells were treated with compound 1 (1  $\mu$ M), 2 (6  $\mu$ M), 3 (1  $\mu$ M), and 32 (1  $\mu$ M) for 2 h, followed by extensive washing with PBS. Then, cells were stimulated with IL-15 for 30 min, lysed, and subjected to standard western blotting.

10-JAKs-STAT3 pathway,<sup>18</sup> but MCP-1 signaling was not mediated by JAKs. Given that compound 32 selectively inhibited JAK3 but not JAK1, we evaluated levels of inflammation cytokines by PBMCs after LPS or IL-6 stimulation. In LPS-challenged PBMCs, the production of IL-6 and TNF- $\alpha$  was significantly inhibited by 100 nM compound 32 and 3, which were significantly more potent than compound 2 (Figure 7A,B). In sharp contrast, the pan-inhibitor 1 significantly increased LPS-induced IL-6 production because of the inhibition of IL-10 feedback signaling. This observation was consistent with the reported data.<sup>18,19</sup> Compounds 1, 2, 3, and 32 did not inhibit IL-6-induced MCP-1 production (not mediated by JAK signaling pathways). These results demonstrated that compound 32 can play an important role in modulating cytokine production through inhibiting the JAK3 signaling pathway.

**Pharmacokinetic Property Evaluation.** We evaluated the pharmacokinetic (PK) properties of compound 32 in mice following intravenous and oral administration (Table 5). Upon 5 mg/kg oral delivery, compound 32 exhibited a reasonable PK profile with a  $t_{1/2}$  of 1.66 h, area under curve (AUC) of 608 ng·h/mL, and moderate bioavailability of 24.4%. These data

suggested that compound 32 could be a useful probe for cellular and animal studies.

**Table 5.** PKs Study of Compound 32 in ICR Mice<sup>a</sup>

Compound 32	iv (2 mg/kg)	po (5 mg/kg)
AUC <sub>0-t</sub> (ng·h/mL)	995 $\pm$ 181	578 $\pm$ 47
AUC <sub>0-<math>\infty</math></sub> (ng·h/mL)	997 $\pm$ 181	608
$T_{1/2}$ (h)	0.44 $\pm$ 0.02	1.66 $\pm$ 1.06
$V_z$ (L/kg)	1.3 $\pm$ 0.21	18.8 $\pm$ 10.06
CL (mL min <sup>-1</sup> kg <sup>-1</sup> )	34.1 $\pm$ 5.62	138.47 $\pm$ 16.3
MRT (h)	0.48 $\pm$ 0.05	1.51 $\pm$ 0.69
bioavailability (%)		24.4

<sup>a</sup>PKs measured by the analysis of plasma concentrations at indicated time points. Data represent mean concentration in plasma ( $n = 3$ ), following a single 2.0 mg/kg intravenous dose and 5 mg/kg oral dose.

## CHEMISTRY

The preparation of compounds was depicted in Schemes 1–. Compounds bearing a strong electron-withdrawing trifluoromethyl group and nitro group were synthesized following a general procedure (Scheme 1). Commercially available compound 37 was converted to the corresponding amide 38. Ring closure with indolyl-oxo-acetic acid ester 39 or substituted indolyl-oxo-acetic acid esters 43 (Scheme 2) led to key intermediates 40 or 44. Reaction with Boc-protected cyclic or linear amines provided 41 or 45 (Schemes 1 and 2). After removing the protection groups, 41 or 45 were coupled with acyl chloride or acid to yield the corresponding final compounds. Regarding compounds with neutral or electron-donating groups on the phenyl group, the preparation procedure was depicted in Scheme 3. Phenylacetic acids were first coupled to Boc-protected piperazine by Buchwald–Hartwig amination to yield 47. The amide conversion, ring closure, removal of protection groups, and amide bond coupling were similarly performed. The synthetic procedure of compound 34 was depicted in Scheme 4. 51 was converted to 52 by treatment with a solution of indole and ethyl-

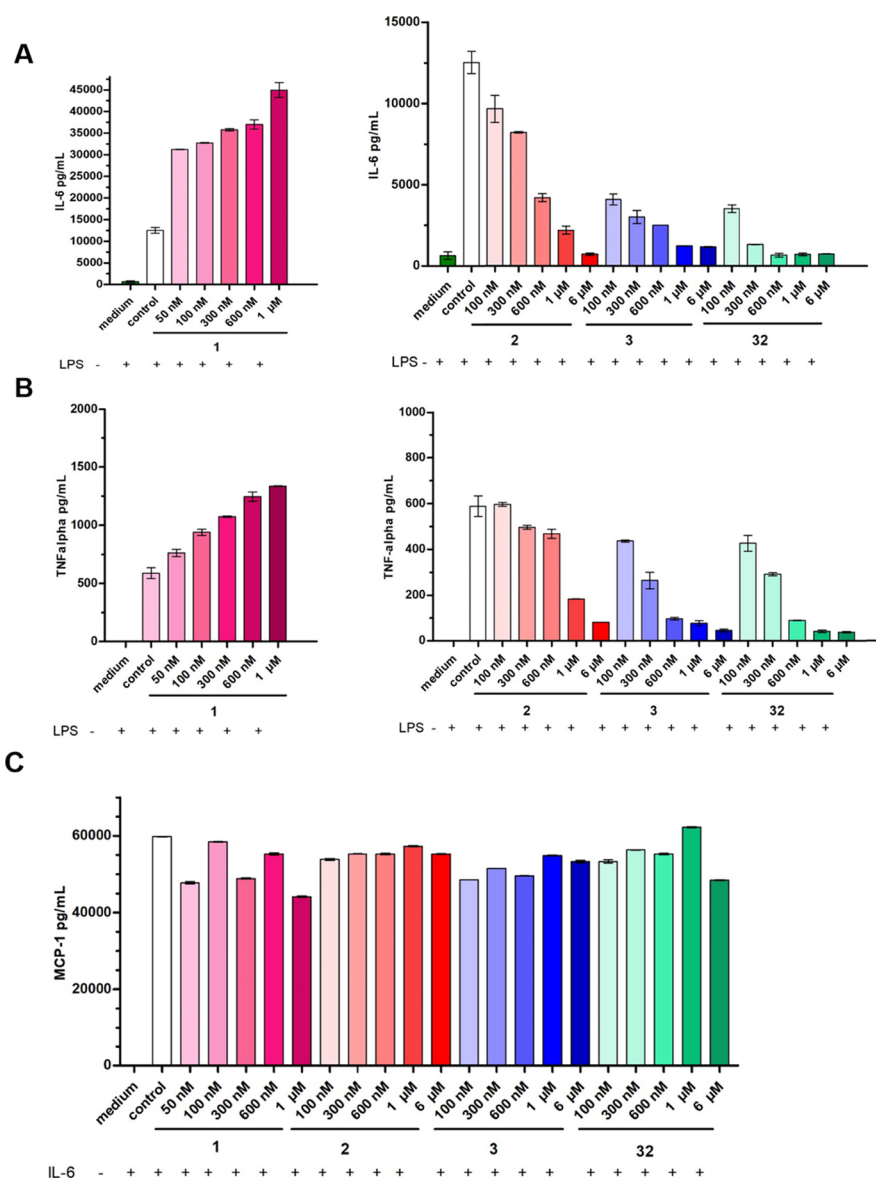


**Figure 7.** Compound 32 selectively inhibited LPS-induced proinflammatory cytokine production by preserving IL-10 suppression. In PBMCs, LPS-induced IL-6 (A) and TNF- $\alpha$  (B) were enhanced in the presence of 1 but reduced in the presence of compound 2, 3, and 32. Compound 1, 2, 3, and 32 did not inhibit IL-6-induced MCP-1 production (C). Error bars indicate standard deviation of technical replicates. Data are representative of two independent experiments.

magnesium bromide in tetrahydrofuran (THF); then displacement with Boc-protected amine gave 53. After removing the Boc protection group, 53 was coupled with acyl chloride to provide the final compound 34. The detailed synthetic experiments are provided in the [Supporting Information](#).

## CONCLUSIONS

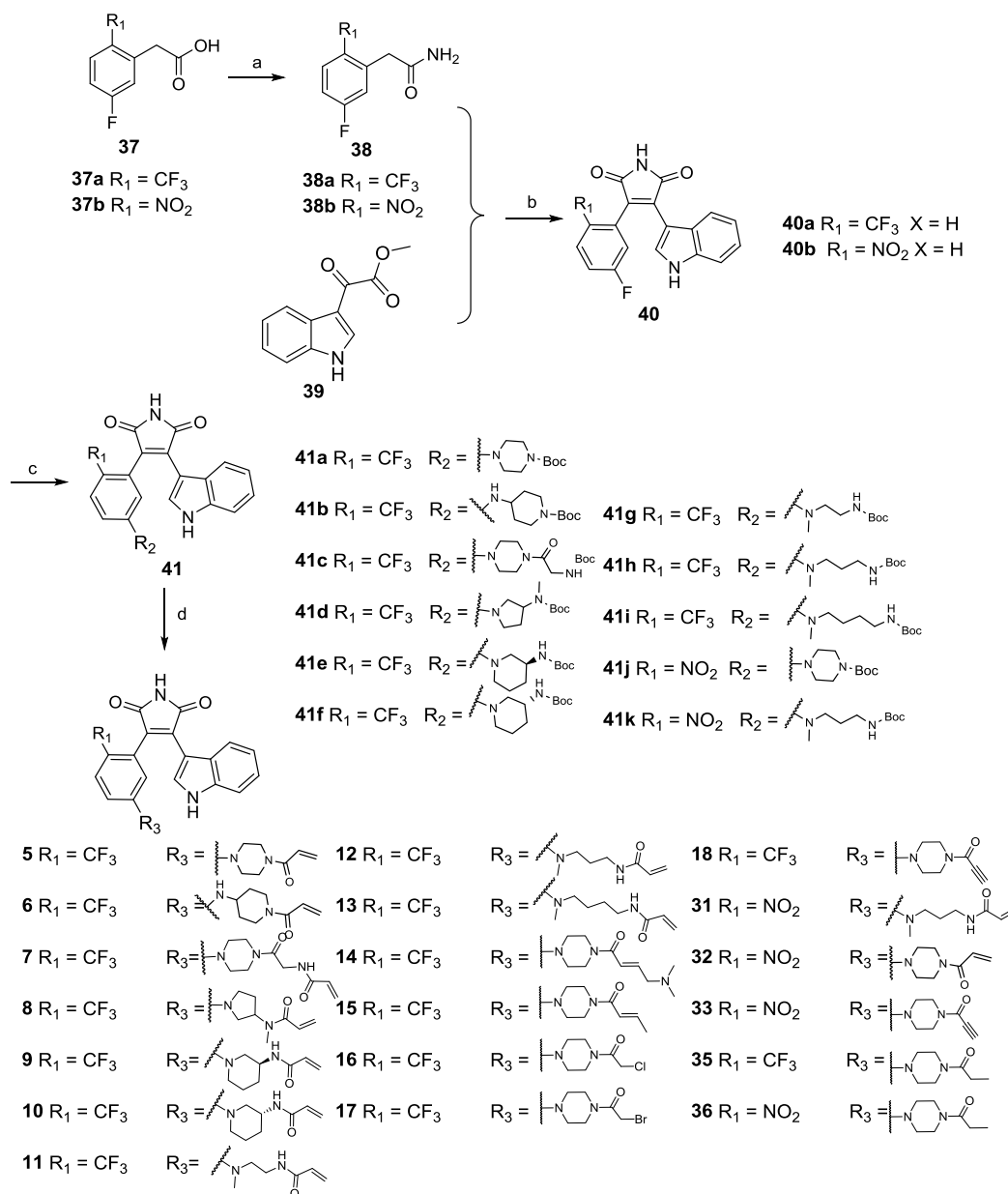
Compound 2 is a highly selective inhibitor within the JAK family but lacking potency in cellular assays, which was considered to suggest that specific inhibition of JAK3 alone was not sufficient to block the common- $\gamma$  chain signaling. To overcome the competition of high ATP concentrations in live cells, we developed a series of phenyl-indolyl maleimide-based covalent inhibitors. Although the initial compound 5 was observed to covalently and irreversibly bind to JAK3, competition with high cellular concentrations of ATP precluded its usefulness as a tool molecule. By fine-tuning noncovalent interactions between the inhibitors and kinase,

compound 32 was discovered. Compound 32 was much more potent than 2 in both enzymatic (1 mM ATP) and cellular assays and presented a high selectivity within the JAK family. Cellular experiments with this compound suggest that inhibiting JAK3 alone strongly inhibits IL-15-mediated signaling. Further in vivo studies with compound 32 are ongoing.

This work also indicates that the simple formation of covalent bond alone may not be sufficient for kinase inhibitors to overcome competition with cellular levels of ATP. Noncovalent interactions should also be carefully optimized for covalent kinase inhibitors to achieve effective potency in native environments.

## EXPERIMENTAL SECTION

**General Methods.** All reagents were purchased commercially and used without further purification, unless otherwise stated. All yields refer to chromatographic yields. Anhydrous dimethyl formamide (DMF) was distilled from calcium hydride. Brine refers to a saturated

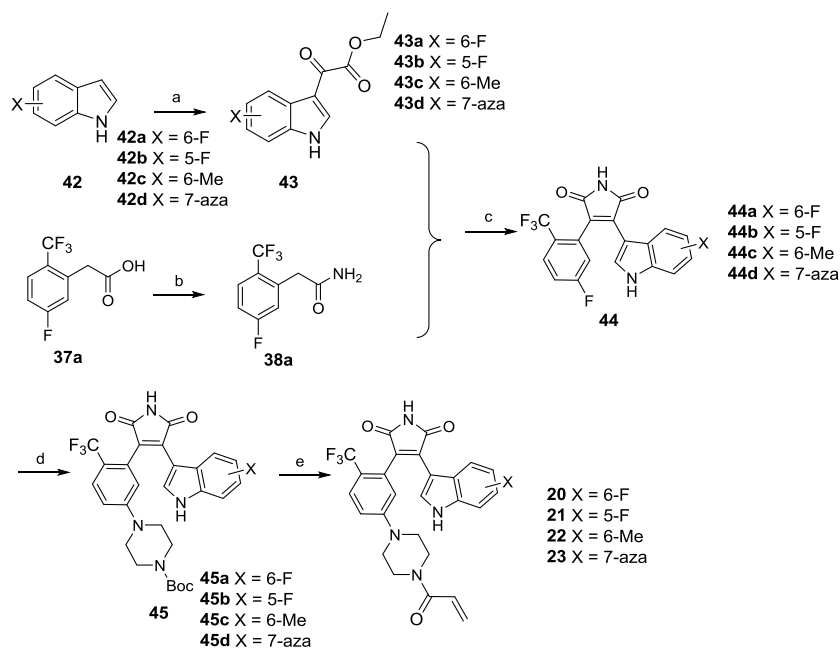
Scheme 1. <sup>4</sup> Synthesis of Compounds 5–18 and 31–36<sup>4a</sup>

<sup>a</sup>Reagents and conditions: (a) (i) CDI, DMF, rt, 0.5 h and (ii)  $\text{NH}_3$  (7 N) in MeOH, rt, 1 h, (75%); (b)  $t\text{BuOK}$ , THF, 0 to 10 °C, 40 min (60–70%); (c) piperazine, or amines DMSO, 150 °C, overnight (70–80%); and (d) (i) TFA/DCM rt, 10 min and (ii) acryloyl chloride, THF,  $\text{H}_2\text{O}$ , 0 °C to rt, 1 h, (80–90%) or carboxylic acid, HATU, DIEA, DMF (for **14**, **15**, **18**, and **33**).

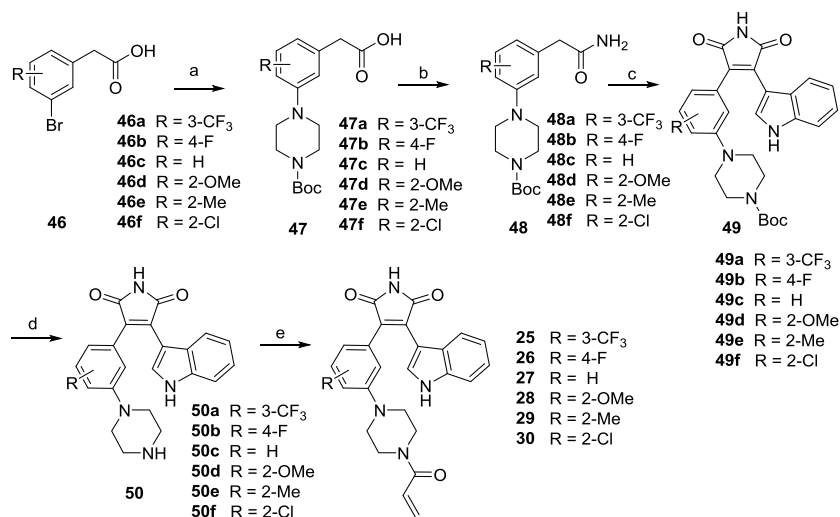
solution of sodium chloride in distilled water. Reactions were monitored by thin-layer chromatography performed on 0.25 mm Yantai silica gel plates (HSGF254) using UV light as a visualizing agent. Flash column chromatography was performed using Yantai silica gel (ZCX-II, particle size 0.048–0.075 mm).  $^1\text{H}$  NMR and  $^{13}\text{C}$  NMR spectra were recorded on a Bruker ADVANCE 400 ( $^1\text{H}$ : 400 MHz,  $^{13}\text{C}$ : 100 MHz) or Bruker ADVANCE 300 ( $^1\text{H}$ : 300 MHz,  $^{13}\text{C}$ : 75 MHz) spectrometer at ambient temperature with chemical shift values in ppm relative to TMS ( $\delta_{\text{H}}$  0.00 and  $\delta_{\text{C}}$  0.00), dimethyl sulfoxide (DMSO) ( $\delta_{\text{H}}$  2.50 and  $\delta_{\text{C}}$  39.52), or methanol ( $\delta_{\text{H}}$  3.31 and  $\delta_{\text{C}}$  49.00) serving as standards. Data are reported as follows: chemical shift, multiplicity (s = singlet, d = doublet, t = triplet, q = quartet, br = broad, and m = multiplet), coupling constants, and number of protons. High-resolution mass spectrometry (HRMS) was performed via electrospray ionization (ESI) sources. Compound purity was determined by HPLC chromatograms acquired on an Agilent 1200 HPLC or 1260 HPLC. Analyses were conducted using an Agilent

PN959990-902 Eclipse Plus C18 250 mm  $\times$  4.6 mm column and a water–MeCN gradient with MeCN from 70 to 30% in 15 min. Detection was measured at 254 nm, and the average peak area was used to determine purity. All of the compounds were determined to be >95% pure.

**Synthesis of 3-(5-(4-Acryloylpiperazin-1-yl)-2-(trifluoromethyl)phenyl)-4-(1H-indol-3-yl)-1H-pyrrole-2,5-dione (5).** *Step 1:* 2-(5-Fluoro-2-(trifluoromethyl)phenyl)acetamide (**38a**). CDI (1.0 g, 4.5 mmol) was added to a solution of 2-(5-fluoro-2-(trifluoromethyl)phenyl)acetic acid in 4 mL of DMF. After stirring for 0.5 h at room temperature (rt),  $\text{NH}_3$  (3.6 mL, 7 N in methanol solution) was added and allowed to stir for another 1 h at rt. The solvent was evaporated and ethyl acetate (2  $\times$  120 mL) was used to extract the product. The combined organic layer was dried over  $\text{Na}_2\text{SO}_4$  and evaporated to give a white residue that was purified by flash column chromatography on silica (80% PE in ethyl acetate ~50% PE in ethyl acetate) to give a white solid (0.73 g, 73%).  $^1\text{H}$

Scheme 2. <sup>4</sup> Synthesis of Compounds 20–23<sup>a</sup>

<sup>a</sup>Reagents and conditions: (a) ethyl 2-chloro-2-oxoacetate, Et<sub>2</sub>AlCl, DCM, 2 h, 0 °C, (50–60%); (b) (i) CDI, DMF, rt, 0.5 h and (ii) NH<sub>3</sub> (7 N) in MeOH, rt, 1 h (75%); (c) <sup>t</sup>BuOK, THF, 0 to 10 °C, 40 min (60–70%); (d) piperazine, DMSO, 150 °C, overnight (70–80%); and (e) (i) TFA/DCM rt, 10 min and (ii) acryloyl chloride, THF, H<sub>2</sub>O, 0 °C to rt, 1 h (80–90%).

Scheme 3. Synthesis of Compounds 25–30<sup>a</sup>

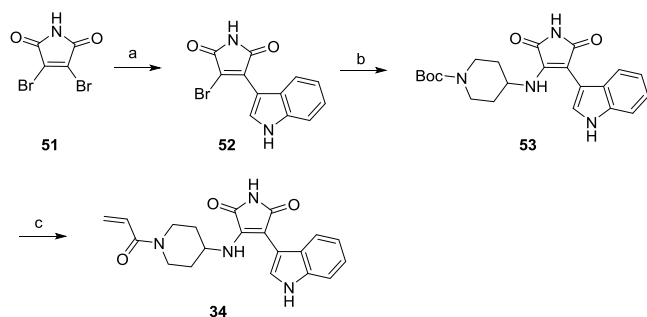
<sup>a</sup>Reagents and conditions: (a) JohnPhos or RuPhos, Pd<sub>2</sub>(dba)<sub>3</sub>, NaO<sup>t</sup>Bu, PhMe or DMF, microwave, 110 °C, 1 h (40–50%); (b) (i) CDI, DMF, rt, 0.5 h; (ii) NH<sub>3</sub> (7 N) in MeOH, rt, 1 h, (75%); (c) <sup>t</sup>BuOK, THF, 0 to 10 °C, 40 min (60–70%); (d) TFA/DCM rt, 10 min; and (e) acryloyl chloride, THF, H<sub>2</sub>O, 0 °C to rt, 1 h (80–90%).

NMR (400 MHz, DMSO-*d*<sub>6</sub>): δ 7.75 (dd, *J* = 8.7, 5.6 Hz, 1H), 7.52 (s, 1H), 7.32 (m, 2H), 7.03 (s, 1H), 3.66 (s, 2H); MS (ESI): *m/z* 222.0 (*M* + H)<sup>+</sup>.

**Step 2:** 3-(5-Fluoro-2-(trifluoromethyl)phenyl)-4-(1H-indol-3-yl)-1H-pyrrole-2,5-dione (**40a**). At 0 °C, <sup>t</sup>BuOK (5.5 mL, 1 M in THF) was added to a solution of **38a** (0.30 g, 1.35 mmol) and **39** (0.41 g, 2.02 mmol) in THF (8 mL). The solution was stirred for 45 min at 10 °C, HCl (5 N) was added to adjust pH to 6, the solvent was removed, the mixture was extracted with ethyl acetate, and the combined organic phase was dried over Na<sub>2</sub>SO<sub>4</sub>. The solvent was removed and the residue was purified by flash column chromatography on silica (90% PE in ethyl acetate ~80% PE in ethyl acetate) to **40a**, a yellow solid (0.35 g, 66%). <sup>1</sup>H NMR (400 MHz, DMSO-*d*<sub>6</sub>): δ 11.99 (s, 1H),

11.23 (s, 1H), 8.02 (d, *J* = 3.0 Hz, 1H), 7.97 (dd, *J* = 8.9, 5.4 Hz, 1H), 7.60–7.52 (m, 1H), 7.49–7.38 (m, 2H), 7.07 (ddd, *J* = 8.1, 7.0, 1.1 Hz, 1H), 6.75 (ddd, *J* = 8.2, 7.1, 1.1 Hz, 1H), 6.46 (d, *J* = 8.3 Hz, 1H). <sup>13</sup>C NMR (101 MHz, DMSO): δ 172.48, 172.01, 165.30, 162.80, 137.08, 136.25, 132.67, 126.18, 125.48, 125.25, 122.91, 120.95, 120.56, 120.19, 119.96, 117.31, 117.09, 112.94, 105.14. MS (ESI): *m/z* 375.1 (*M* + H)<sup>+</sup>.

**Step 3:** *tert*-Butyl-4-(3-(4-(1H-indol-3-yl)-2,5-dioxo-2,5-dihydro-1H-pyrrol-3-yl)-4-(trifluoromethyl)phenyl)piperazine-1-carboxylate (**41a**). Boc-piperazine (0.64 g, 3.45 mmol) was added to a solution of **40a** (0.30 g, 0.80 mmol) in DMSO (2 mL) and the mixture was refluxed overnight at 150 °C. The mixture was diluted and extracted with ethyl acetate, washed with water and brine, and the organic phase

Scheme 4. Synthesis of Compound 34<sup>a</sup>

<sup>a</sup>Reagents and conditions: (a) indole, EtMgBr in Et<sub>2</sub>O, THF, reflux (86%); (b) Boc-protected amine, DIEA, DMF, 100 °C; and (c) (i) TFA/DCM, rt, 10 min and (ii) acryloyl chloride, THF, H<sub>2</sub>O, 0 °C to rt, 1 h (80%).

was dried over Na<sub>2</sub>SO<sub>4</sub>. The solvent was removed and the residue was purified by flash column chromatography on silica (90% PE in ethyl acetate ~60% PE in ethyl acetate) to give **41a**, a yellow solid (0.22 g, 52%). <sup>1</sup>H NMR (400 MHz, DMSO-*d*<sub>6</sub>): δ 11.88 (s, 1H), 11.10 (s, 1H), 7.95 (d, *J* = 2.9 Hz, 1H), 7.64 (d, *J* = 9.0 Hz, 1H), 7.38 (d, *J* = 8.1 Hz, 1H), 7.18–7.10 (m, 1H), 7.09–6.99 (m, 1H), 6.92 (d, *J* = 2.6 Hz, 1H), 6.72 (dd, *J* = 8.2, 7.0 Hz, 1H), 6.61 (d, *J* = 8.2 Hz, 1H), 3.34–3.22 (m, 5H), 3.24–3.09 (m, 4H), 1.38 (s, 9H). <sup>13</sup>C NMR (101 MHz, DMSO): δ 172.85, 172.40, 154.34, 152.82, 136.97, 135.64, 132.09, 131.86, 131.85, 128.70, 128.42, 126.50, 126.50, 125.39, 125.38, 122.69, 121.37, 120.70, 117.97, 114.87, 112.64, 105.55, 79.57, 49.00, 47.32, 30.63, 29.52, 28.55. MS (ESI): *m/z* 541.2 (M + H)<sup>+</sup>.

**Step 4:** 3-(5-(4-Acryloylpiperazin-1-yl)-2-(trifluoromethyl)phenyl)-4-(1H-indol-3-yl)-1H-pyrrole-2,5-dione (**5**). Trifluoroacetyl acid (TFA) (2 mL) was added to a solution of **41a** (0.10 g, 0.18 mmol) in DCM (2.0 mL) and the mixture was stirred at rt for 15 min. TFA and the solvent were evaporated, and the residue was used in the next step without further purification. The residue was dissolved in a mixture of THF (2 mL) and water (1 drop), followed by adding DIEA (0.1 mL) and acryloyl chloride (24 μL). The resulting solution was stirred at rt for 10 min. After removing the solvent, the mixture was extracted with ethyl acetate, washed with brine, and the organic phase was dried over Na<sub>2</sub>SO<sub>4</sub>. The solvent was removed and the residue was purified by flash column chromatography on silica (1% methanol in DCM ~1.5% methanol in DCM) to give a yellow solid **5** (73 mg, 82%). <sup>1</sup>H NMR (400 MHz, DMSO-*d*<sub>6</sub>): δ 11.88 (d, *J* = 3.0 Hz, 1H), 11.11 (s, 1H), 7.96 (d, *J* = 2.6 Hz, 1H), 7.65 (d, *J* = 8.9 Hz, 1H), 7.38 (d, *J* = 8.1 Hz, 1H), 7.18–7.10 (m, 1H), 7.08–7.00 (m, 1H), 6.96 (d, *J* = 2.5 Hz, 1H), 6.76 (m, 2H), 6.65 (d, *J* = 8.3 Hz, 1H), 6.11 (dd, *J* = 16.6, 2.4 Hz, 1H), 5.68 (dd, *J* = 10.4, 2.4 Hz, 1H), 3.66–3.46 (m, 4H), 3.23 (m, 4H). <sup>13</sup>C NMR (101 MHz, DMSO): δ 172.64, 172.20, 164.62, 152.49, 136.73, 135.43, 131.85, 131.65, 128.49, 128.34, 127.86, 126.28, 125.18, 123.57, 122.50, 121.15, 120.51, 117.67, 114.54, 112.42, 105.35, 47.58, 47.01, 44.37, 40.90, 39.98. HRMS (ESI): *m/z* calcd for C<sub>26</sub>H<sub>22</sub>F<sub>3</sub>N<sub>4</sub>O<sub>3</sub> [M + H]<sup>+</sup>, 495.1644; found, 495.1678.

Compounds **6–18** and **31–36** were prepared following the similar synthetic procedure of compound **5**. Detailed experimental procedure and spectral data are present in the [Supporting Information](#).

**Synthesis of 3-(5-(4-Acryloylpiperazin-1-yl)-2-(trifluoromethyl)phenyl)-4-(6-fluoro-1H-indol-3-yl)-1H-pyrrole-2,5-dione (**20**).** **Step 1:** Ethyl 2-(6-fluoro-1H-indol-3-yl)-2-oxoacetate (**43a**). To a solution of **42a** (0.50 g, 3.7 mmol) in DCM (40 mL) was added 5.6 mL of Et<sub>2</sub>AlCl (1 M in hexane) at 0 °C. The mixture was stirred at 0 °C for 30 min. To this solution was added acetyl chloride (0.76 mL, 5.5 mmol) as dropwise at 0 °C. The resulting solution was stirred at 0 °C for 2 h, then ice water was added to quench the reaction. The solvent was evaporated and ethyl acetate (2 × 120 mL) was used to extract the product. The combined organic layer was dried over Na<sub>2</sub>SO<sub>4</sub> and evaporated to give a dark residue that was purified by flash column chromatography on silica (90% PE

in ethyl acetate ~60% PE in ethyl acetate) to give compound **43a** (0.38 g, 50%) as a pale solid. <sup>1</sup>H NMR (400 MHz, DMSO-*d*<sub>6</sub>): δ 12.41 (s, 1H), 8.44 (s, 1H), 8.14 (dd, *J* = 8.7, 5.5 Hz, 1H), 7.35 (dd, *J* = 9.5, 2.4 Hz, 1H), 7.13 (ddd, *J* = 9.8, 8.7, 2.4 Hz, 1H), 4.35 (q, *J* = 7.1 Hz, 2H), 1.33 (t, *J* = 7.1 Hz, 3H). MS (ESI): *m/z* 236.1 (M + H)<sup>+</sup>.

**Step 2:** 3-(6-Fluoro-1H-indol-3-yl)-4-(5-fluoro-2-(trifluoromethyl)phenyl)-1H-pyrrole-2,5-dione (**44a**). At 0 °C, <sup>t</sup>BuOK (4 mL, 1 M in THF) was added to a solution of **38a** (0.19 g, 0.85 mmol) and **43a** (0.3 g, 1.3 mmol) in THF (4 mL). The solution was stirred for 1 h at 10 °C, HCl (5 N) was added to adjust pH to 6, the solvent was removed, the mixture was extracted with ethyl acetate, and the organic phase was dried with Na<sub>2</sub>SO<sub>4</sub>. The solvent was removed and the residue was purified by flash column chromatography on silica (90% PE in ethyl acetate ~80% PE in ethyl acetate) to give **44a** (0.25 g, 75% yield), a yellow solid. <sup>1</sup>H NMR (400 MHz, DMSO-*d*<sub>6</sub>): δ 12.06 (s, 1H), 11.26 (s, 1H), 8.03 (d, *J* = 3.1 Hz, 1H), 8.00 (dd, *J* = 8.9, 5.4 Hz, 1H), 7.60 (m, 1H), 7.49 (dd, *J* = 9.2, 2.7 Hz, 1H), 7.42 (dd, *J* = 8.9, 4.8 Hz, 1H), 6.94 (m, 1H), 6.14 (dd, *J* = 11.1, 2.5 Hz, 1H). MS (ESI): *m/z* 393.0 (M + H)<sup>+</sup>.

**Step 3:** *tert*-Butyl 4-(3-(4-(6-fluoro-1H-indol-3-yl)-2,5-dioxo-2,5-dihydro-1H-pyrrol-3-yl)-4-(trifluoromethyl)phenyl)piperazine-1-carboxylate (**45a**). Boc-piperazine (0.53 g, 2.84 mmol) was added to a solution of **44a** (0.26 g 0.66 mmol) in DMSO (2 mL) and the mixture was refluxed overnight at 150 °C. The mixture was extracted with ethyl acetate, washed with water and brine, and the organic phase was dried over Na<sub>2</sub>SO<sub>4</sub>. The solvent was removed and the residue was purified by flash column chromatography on silica (90% PE in ethyl acetate ~60% PE in ethyl acetate) to give **45a** (0.12 g, 30%), a yellow solid. <sup>1</sup>H NMR (400 MHz, DMSO-*d*<sub>6</sub>): δ 11.87 (s, 1H), 11.13 (s, 1H), 7.89 (s, 1H), 7.64 (d, *J* = 9.0 Hz, 1H), 7.17 (dd, *J* = 9.5, 2.3 Hz, 1H), 7.13 (dd, *J* = 8.8, 2.6 Hz, 1H), 6.94 (d, *J* = 2.6 Hz, 1H), 6.70–6.57 (m, 2H), 3.33–3.25 (m, 4H), 3.22 (m, 4H), 1.39 (s, 9H). MS (ESI): *m/z* 559.2 (M + H)<sup>+</sup>.

**Step 4:** 3-(5-(4-Acryloylpiperazin-1-yl)-2-(trifluoromethyl)phenyl)-4-(6-fluoro-1H-indol-3-yl)-1H-pyrrole-2,5-dione (**20**). TFA (1 mL) was added to a solution of **45a** (0.10 g 0.18 mmol) in DCM (1 mL) and the mixture was stirred at rt for 15 min. TFA and the solvent were evaporated, and the residue was used in the next step without further purification. The residue was dissolved in a mixture of THF (2 mL) and water (1 drop), followed by adding DIEA (0.1 mL, 0.54 mmol) and acryloyl chloride (24 μL, 0.27 mmol). The resulting solution was stirred at rt for 10 min. After removing the solvent, the mixture was extracted with ethyl acetate, washed with brine, and the organic phase was dried over Na<sub>2</sub>SO<sub>4</sub>. The solvent was removed, and the residue was purified by flash column chromatography on silica (1% methanol in DCM ~1.5% methanol in DCM) to give **20** (74 mg, 80%), a yellow solid. <sup>1</sup>H NMR (400 MHz, DMSO-*d*<sub>6</sub>): δ 11.86 (s, 1H), 11.12 (s, 1H), 7.87 (s, 1H), 7.64 (d, *J* = 9.0 Hz, 1H), 7.21–7.08 (m, 2H), 6.97 (d, *J* = 2.3 Hz, 1H), 6.78 (m, 1H), 6.69 (m, 1H), 6.62 (m, 1H), 6.11 (dd, *J* = 16.7, 2.3 Hz, 1H), 5.68 (dd, *J* = 10.4, 2.3 Hz, 1H), 3.55 (m, 4H), 3.24 (m, 4H). <sup>13</sup>C NMR (101 MHz, DMSO-*d*<sub>6</sub>): δ 172.70, 172.30, 164.88, 158.20, 152.82, 137.14, 137.02, 135.41, 132.57, 129.48, 128.63, 128.05, 122.60, 122.51, 122.17, 117.72, 114.79, 109.16, 108.92, 105.65, 98.84, 98.59, 47.75, 47.16, 44.65, 41.14. HRMS (ESI): *m/z* calcd for C<sub>26</sub>H<sub>21</sub>F<sub>4</sub>N<sub>4</sub>O<sub>3</sub> [M + H]<sup>+</sup>, 513.1550; found, 513.1559. Purity: 99.2%.

Compounds **21–23** were prepared following a similar synthetic procedure of compound **20**. Detailed spectral data are present in the [Supporting Information](#). **42a–42d** were purchased from Bide Pharmatech Ltd.

**Synthesis of 3-(5-(4-acryloylpiperazin-1-yl)-2-methoxyphenyl)-4-(1H-indol-3-yl)-1H-pyrrole-2,5-dione (**28**).** **Step 1:** 2-(5-(4-*tert*-Butoxycarbonyl)piperazin-1-yl)-2-methoxyphenyl)acetic acid (**47d**). **46d** (0.50 g, 2.04 mmol), *tert*-butyl piperazine-1-carboxylate (0.49 g, 2.65 mmol), sodium *tert*-butoxide (0.59 g, 2.65 mmol), 2-(*di*-*tert*-butylphosphino)biphenyl (JohnPhos, 0.16 g, 0.41 mmol), and Pd<sub>2</sub>(dba)<sub>3</sub> (0.19 g, 0.20 mmol) were taken up in PhMe (15 mL) in a microwave vial and purged with N<sub>2</sub> for 5 min. The vial was capped and heat to 110 °C for 1 h. After cooling to room

temperature, the mixture was adjusted to a pH of 5 and extracted with ethyl acetate, washed with brine, and the organic phase was dried over  $\text{Na}_2\text{SO}_4$ . The solvent was removed and the residue was purified by flash column chromatography on silica (80% PE in ethyl acetate ~50% PE in ethyl acetate) to give a white solid **47d** (0.35 g, 49%).  $^1\text{H}$  NMR (500 MHz,  $\text{DMSO}-d_6$ ):  $\delta$  6.87–6.85 (m, 1H), 6.84 (s, 1H), 6.82 (d,  $J = 2.8$  Hz, 1H), 3.68 (s, 3H), 3.45 (m, 2H), 3.44 (m, 4H), 2.94 (m, 4H).  $^{13}\text{C}$  NMR (126 MHz,  $\text{DMSO}$ ):  $\delta$  173.04, 154.32, 152.01, 145.32, 124.49, 121.12, 116.45, 111.74, 79.40, 56.13, 50.34, 36.23, 28.53. MS (ESI):  $m/z$  351.2 ( $\text{M} + \text{H}$ ) $^+$ .

**Step 2: tert-Butyl 4-(3-(2-amino-2-oxoethyl)-4-methoxyphenyl)piperazine-1-carboxylate (48d).** CDI (0.29 g, 1.29 mmol) was added to a solution of **47d** (0.30 g, 0.86 mmol) in 2 mL of DMF. After stirring for 0.5 h at room temperature,  $\text{NH}_3$  (0.6 mL 7 N in methanol solution) was added and allowed to stir for another 1 h at rt. The solvent was evaporated, and ethyl acetate (2  $\times$  120 mL) was used to extract the product. The combined organic layer was dried over  $\text{Na}_2\text{SO}_4$  and evaporated to give a white residue that was purified by flash column chromatography on silica (80% PE in ethyl acetate ~50% PE in ethyl acetate) to give a white solid **48d** (0.22 g 70%).  $^1\text{H}$  NMR (500 MHz,  $\text{DMSO}-d_6$ ):  $\delta$  7.17 (s, 1H), 6.92–6.69 (m, 4H), 3.69 (s, 3H), 3.69–3.43 (m, 4H), 3.31 (s, 2H), 2.95–2.93 (m, 4H), 1.42 (s, 9H).  $^{13}\text{C}$  NMR (126 MHz,  $\text{DMSO}$ ):  $\delta$  172.60, 154.31, 151.93, 145.33, 125.50, 120.96, 116.16, 111.76, 79.39, 56.15, 50.40, 37.30, 28.53. MS (ESI):  $m/z$  350.2 ( $\text{M} + \text{H}$ ) $^+$ .

**Step 3: tert-Butyl 4-(3-(4-(1H-indol-3-yl)-2,5-dioxo-2,5-dihydro-1H-pyrrol-3-yl)-4-methoxyphenyl)piperazine-1-carboxylate (49d).** At 0  $^\circ\text{C}$ ,  $t\text{-BuOK}$  (2.2 mL, 1 M in THF) was added to a solution of **48d** (0.20 g, 0.57 mmol) and **39** (0.17 g, 0.85 mmol) in THF (4 mL). The solution was stirred for 2 h at 10  $^\circ\text{C}$ , HCl (5 N) was added to adjust pH to 5, the solvent was removed, the mixture was extracted with ethyl acetate, and the organic phase was dried with  $\text{Na}_2\text{SO}_4$ . The solvent was removed, and the residue was used in the next step without further purification. MS (ESI):  $m/z$  503.2 ( $\text{M} + \text{H}$ ) $^+$ .

**Step 4: 3-(1H-Indol-3-yl)-4-(2-methoxy-5-(piperazin-1-yl)-phenyl)-1H-pyrrole-2,5-dione (50d).** TFA (2 mL) was added to a solution of **49d** (0.12 g, 0.24 mmol) in DCM (2 mL) and the mixture was stirred at rt for 15 min. TFA and the solvent were evaporated, the mixture was extracted with ethyl acetate, washed by  $\text{NaHCO}_3$  and brine, and the organic phase was dried with  $\text{Na}_2\text{SO}_4$ . The solvent was removed, and the residue was purified by flash column chromatography on silica (2% methanol in DCM ~10% methanol in DCM) to give a yellow solid **50d** (0.15 g, 52% for two steps).  $^1\text{H}$  NMR (400 MHz,  $\text{DMSO}-d_6$ ):  $\delta$  11.80 (s, 1H), 7.91 (s, 1H), 7.37 (d,  $J = 8.1$  Hz, 1H), 7.02 (ddd,  $J = 8.2, 7.0, 1.1$  Hz, 1H), 6.95 (dd,  $J = 9.0, 3.0$  Hz, 1H), 6.88 (d,  $J = 9.1$  Hz, 1H), 6.78 (d,  $J = 2.9$  Hz, 1H), 6.65 (ddd,  $J = 8.2, 7.0, 1.1$  Hz, 1H), 6.51–6.41 (m, 1H), 3.26 (s, 3H), 2.89–2.81 (m, 4H), 2.80–2.78 (m, 4H).  $^{13}\text{C}$  NMR (101 MHz,  $\text{DMSO}$ ):  $\delta$  173.08, 172.67, 152.06, 145.93, 136.87, 134.69, 130.87, 128.29, 125.38, 122.39, 121.29, 121.12, 120.23, 119.96, 118.58, 113.08, 112.38, 106.29, 55.97, 50.91, 45.78. MS (ESI):  $m/z$  403.2 ( $\text{M} + \text{H}$ ) $^+$ .

**Step 5: 3-(5-(4-Acryloylpiperazin-1-yl)-2-methoxyphenyl)-4-(1H-indol-3-yl)-1H-pyrrole-2,5-dione (28).** **50d** (0.10 g, 0.24 mmol) was dissolved in a mixture of THF (2 mL) and water (1 drop), followed by adding DIEA (0.16 mL, 0.96 mmol) and acryloyl chloride (0.03 mL, 0.36 mmol). The resulting solution was stirred at rt for 10 min. After removing the solvent, the mixture was extracted with ethyl acetate, washed with brine, and the organic phase was dried over  $\text{Na}_2\text{SO}_4$ . The solvent was removed, and the residue was purified by flash column chromatography on silica (1% methanol in DCM ~1.5% methanol in DCM) to give a yellow solid **28** (0.09 g, 82% for two steps).  $^1\text{H}$  NMR (400 MHz,  $\text{DMSO}-d_6$ ):  $\delta$  11.81 (s, 1H), 10.93 (s, 1H), 7.93 (d,  $J = 2.8$  Hz, 1H), 7.38 (d,  $J = 8.1$  Hz, 1H), 7.07–6.98 (m, 2H), 6.92 (d,  $J = 9.0$  Hz, 1H), 6.84 (d,  $J = 2.9$  Hz, 1H), 6.80 (dd,  $J = 16.7, 10.5$  Hz, 1H), 6.66 (t,  $J = 7.3$  Hz, 1H), 6.45 (d,  $J = 8.1$  Hz, 1H), 6.10 (dd,  $J = 16.7, 2.4$  Hz, 1H), 5.68 (dd,  $J = 10.4, 2.4$  Hz, 1H), 3.59 (m, 4H), 3.29 (s, 3H), 2.91 (m, 4H).  $^{13}\text{C}$  NMR (101 MHz,  $\text{DMSO}-d_6$ ):  $\delta$  173.05, 172.62, 164.74, 152.47, 144.97, 136.88, 134.75, 130.96, 128.69, 128.10, 127.93, 125.33, 122.42, 121.25, 121.20, 120.60, 120.26, 119.13, 113.12, 112.42, 106.23, 55.98, 50.83, 50.22,

45.27, 41.73. HRMS (ESI):  $m/z$  calcd for  $\text{C}_{26}\text{H}_{25}\text{N}_4\text{O}_4$  [ $\text{M} + \text{H}$ ] $^+$ , 457.1876; found, 457.1794. Purity: 97.0%.

Compounds **25–30** were prepared following a similar synthetic procedure of compound **28**. Detailed spectral data are present in the Supporting Information. **46a–46f** were purchased from J&K Scientific (Beijing, China).

**Synthesis of 3-((1-Acryloylpiperidin-4-yl)amino)-4-(1H-indol-3-yl)-1H-pyrrole-2,5-dione (34).** **Step 1: 3-Bromo-4-(1H-indol-3-yl)-1H-pyrrole-2,5-dione (52).** In a two-necked flask equipped with a dropping funnel under argon, indole (0.30 g, 1.18 mmol) was dissolved in anhydrous THF (8 mL). A solution of 3 M ethyl magnesium bromide in  $\text{Et}_2\text{O}$  (1.57 mL, 4.71 mmol) was added dropwise into the mixture, which was then heated to reflux for 2 h. After cooling, a solution of **51** (0.55 g, 4.71 mmol) in anhydrous THF (6 mL) was added dropwise over 1 h. Then, the reaction mixture was stirred at rt for 1 h. The mixture was then hydrolyzed to pH = 9 with aqueous HCl solution. After adding saturated aqueous  $\text{NH}_4\text{Cl}$  solution, the aqueous phase was extracted with ethyl acetate. The combined organic layers were then washed with saturated aqueous NaCl, dried over  $\text{Na}_2\text{SO}_4$ , and evaporated under vacuum. The residue was purified by flash column chromatography on silica to yield **52** (0.28 g, 82%), a yellow solid.  $^1\text{H}$  NMR (400 MHz,  $\text{DMSO}-d_6$ ):  $\delta$  12.10 (s, 1H), 11.35 (s, 1H), 8.03 (d,  $J = 2.9$  Hz, 1H), 7.89 (dt,  $J = 8.1, 1.0$  Hz, 1H), 7.51 (dt,  $J = 8.1, 1.0$  Hz, 1H), 7.22 (ddd,  $J = 8.1, 7.0, 1.2$  Hz, 1H), 7.14 (ddd,  $J = 8.1, 7.1, 1.2$  Hz, 1H).  $^{13}\text{C}$  NMR (101 MHz,  $\text{DMSO}$ ):  $\delta$  170.75, 167.99, 138.54, 137.01, 131.54, 125.05, 122.95, 122.77, 120.92, 115.13, 112.84, 104.25. MS (ESI):  $m/z$  291.0 ( $\text{M} + \text{H}$ ) $^+$ .

**Step 2: tert-Butyl 4-((4-(1H-indol-3-yl)-2,5-dioxo-2,5-dihydro-1H-pyrrol-3-yl)amino)piperidine-1-carboxylate (53).** **52** (0.13 g, 0.45 mmol) and piperidin-4-amine (0.18 g, 0.89 mmol) were dissolved in DMSO (1.5 mL), followed by the addition of DIEA (0.15 mL, 0.89 mmol). The mixture was heated at 126  $^\circ\text{C}$  overnight. After cooling, the mixture was diluted with water and extracted with ethyl acetate. The combined organic layers were then washed with brine, dried over  $\text{Na}_2\text{SO}_4$ , and evaporated under vacuum. The residue was purified by flash column chromatography on silica to yield **53** (0.11 g, 60%), a yellow solid.  $^1\text{H}$  NMR (400 MHz,  $\text{DMSO}-d_6$ ):  $\delta$  11.21 (d,  $J = 2.5$  Hz, 1H), 10.34 (s, 1H), 7.40 (d,  $J = 8.1$  Hz, 1H), 7.37–7.27 (m, 2H), 7.14–7.06 (m, 1H), 7.04–6.95 (m, 1H), 6.86 (d,  $J = 9.0$  Hz, 1H), 3.67 (m, 2H), 3.43 (m, 1H), 1.97 (m, 2H), 1.47 (m, 2H), 1.31 (s, 9H), 1.26 (m, 2H).  $^{13}\text{C}$  NMR (101 MHz,  $\text{DMSO}$ ):  $\delta$  173.82, 169.57, 154.19, 143.23, 136.10, 128.71, 126.48, 121.70, 119.91, 119.37, 112.05, 104.59, 100.05, 93.48, 79.22, 50.31, 32.01, 28.52. MS (ESI):  $m/z$  410.1 ( $\text{M} + \text{H}$ ) $^+$ .

**Step 3: 3-((1-Acryloylpiperidin-4-yl)amino)-4-(1H-indol-3-yl)-1H-pyrrole-2,5-dione (34).** TFA (2 mL) was added to a solution of **53** (0.10 g, 0.24 mmol) in DCM (2 mL) and the mixture was stirred at rt for 15 min. TFA and the solvent were evaporated, and the residue was used in the next step without further purification. The residue (0.24 mmol) was dissolved in a mixture of THF (2 mL) and water (1 drop), followed by the addition of DIEA (0.16 mL, 0.96 mmol) and acryloyl chloride (0.03 mL, 0.36 mmol). The resulting solution was stirred at rt for 10 min. After removing the solvent, the mixture was extracted with ethyl acetate and washed with brine. The organic phase was dried over  $\text{Na}_2\text{SO}_4$ . The solvent was removed, and the residue was purified by flash column chromatography on silica (1% methanol in DCM ~1.5% methanol in DCM) to yield a yellow solid **34** (0.08 g, 90% for two steps).  $^1\text{H}$  NMR (400 MHz,  $\text{DMSO}-d_6$ ):  $\delta$  11.23 (s, 1 H), 10.43 (s, 1 H), 7.54–7.20 (m, 3 H), 7.09 (d,  $J = 7.1$  Hz, 1 H), 7.01 (t,  $J = 7.0$  Hz, 1 H), 6.64 (d,  $J = 7.5$  Hz, 1 H), 5.75 (t,  $J = 14.6$  Hz, 1 H), 5.27 (d,  $J = 7.8$  Hz, 1 H), 3.87 (d,  $J = 12.2$  Hz, 1 H), 2.93 (m, 1 H), 2.82 (m, 1 H), 2.56 (m, 1 H), 1.75 (m, 1 H), 1.57 (m, 2 H), 0.84 (m, 1 H).  $^{13}\text{C}$  NMR (101 MHz,  $\text{DMSO}$ ):  $\delta$  173.79, 169.60, 164.78, 142.34, 136.13, 128.48, 128.46, 127.84, 127.35, 126.68, 121.84, 119.96, 119.59, 112.24, 104.14, 50.10, 49.39, 41.81, 30.50, 28.52. HRMS (ESI):  $m/z$  calcd for  $\text{C}_{20}\text{H}_{21}\text{N}_4\text{O}_3$  [ $\text{M} + \text{H}$ ] $^+$ , 365.1614; found, 365.1591. Purity: 99.3%.

**Enzymatic Assay.** Kinases were purchased from Carma Biosciences. The enzymatic activities of JAK3 were assessed using the

homogeneous time-resolved fluorescence (HTRF) KinEase assay with concentrations of ATP at  $K_m$  and 1 mM, separately. ATP Kinase enzymology assays were performed according to the protocols specified by HTRF KinEase assay instructions (Cisbio Bioassays).

**Time-Dependent Assay.** Compound **1**, **3**, and **5** or kinase buffer (positive control) were incubated with recombinant JAK3 for various periods of time (0, 2, 4, 8, 16, 20, 30, or 40 min) before ATP ( $K_m$  or 1 mM), and the substrate was added to initiate the kinase reaction. The stop reactions were kept constant according to HTRF KinEase assays. The according inhibition rate values were plotted versus incubation time using GraphPad Prism software.

**Kinetic Characterization.** The inhibitors were incubated with recombinant JAK3 for different periods of time, whereas durations of enzymatic and stop reactions were kept constant according to HTRF KinEase assays. The starting concentration was dependent on  $IC_{50}$  values of compounds, and concentrations from a threefold dilution series (six data points per  $IC_{50}$  curve) were applied. The enzymatic activity was measured with HTRF KinEase assays. The collected data were fitted as described in the literature<sup>20</sup> to determine  $k_{inact}$  and  $K_i$ . GraphPad Prism was used for curved fitting.

**Cellular Assays.** CTLL-2 cells were deprived of growth factors and starved overnight. Then, cells were incubated with JAK3 inhibitors or DMSO for 2 h at 37 °C. After stimulation with 500 ng/mL IL-2 or 500 ng/mL IL-5 (R&D Systems) for 30 min, cells were collected and lysed in cell lysis buffer containing protease and phosphatase inhibitors. Western blotting analyses were then conducted after separation by SDS/PAGE electrophoresis and transfer to nitrocellulose membranes. Phospho-STAT5, STAT5, and  $\beta$ -actin (all antibodies were from Cell Signaling Technologies) were blotted separately with specific antibodies. The  $EC_{50}$  values were calculated by quantitative stripe gray analysis of pSTAT5 using GraphPad Prism software.

PBMCs were purchased from AllCells. After thawing, PBMCs were resuspended in RPMI-1640 containing 10% FBS overnight and then incubated with JAK3 inhibitors or DMSO for 2 h. After stimulation with IL-2 (500 ng/mL, R&D Systems), IL-15 (500 ng/mL, R&D Systems), IL-6 (600 ng/mL, R&D Systems), or IFN- $\alpha$  (400 ng/mL, R&D Systems) for 30 min, cells were collected and lysed in cell lysis buffer containing protease and phosphatase inhibitors. Western blotting analyses were then conducted after separation by SDS/PAGE electrophoresis and transferred to nitrocellulose membranes. Phospho-STAT5, Phospho-STAT3, and phospho-STAT1 (all from Cell Signaling Tech) were blotted separately with specific antibodies.  $\beta$ -actin was blotted for equal loading.

**Washout Experiment.** CTLL-2 cells were deprived of growth factors and starved overnight and treated with **1**, **2**, **3**, or compound **32** for 2 h. For washout groups, cells were washed extensively with PBS. The nonwashout groups were kept constant as stated above. Cells were stimulated with IL-15 for 30 min, lysed, and subjected to standard Western blot.

**LPS-Induced IL-6 and TNF- $\alpha$  Secretion Assays.** Frozen PBMCs (from AllCells) were thawed in RPMI1640 (Thermo Fisher) containing 10% FBS and recovered overnight at 37 °C. The next day, cells were diluted to  $1 \times 10^6$  cells/mL and seeded (500  $\mu$ L) in 6-well plates. Compounds or DMSO (5  $\mu$ L, serially diluted in DMSO) were added to the plates and incubated with cells for 2 h at 37 °C, followed by stimulation with LPS (5  $\mu$ L, 1  $\mu$ g/mL) and incubation for 24 h at 37 °C in 5% CO<sub>2</sub>. Supernatants were collected for determination of IL-6 and TNF- $\alpha$  levels using human IL-6 or human TNF- $\alpha$  DuoSet ELISA Kits (R&D Systems) according to the manufacturer's instructions.

**In Vivo PKs Study.** Male ICR mice ( $n = 3$ ) were fasted overnight and compound **32** was received as an intravenous dose (2 mg/kg) or via oral gavage (5 mg/kg). Blood samples were collected at 0.08, 0.25, 0.5, 1, 2, 4, 8, and 24 h (iv) and 0.25, 0.5, 1, 2, 4, 8, and 24 h (po). The plasma samples were deproteinized with acetonitrile containing an internal standard. After centrifugation at 4 °C, supernatants were collected for LC/MS/MS analysis.

## ■ ASSOCIATED CONTENT

### 📄 Supporting Information

The Supporting Information is available free of charge on the ACS Publications website at DOI: 10.1021/acs.jmedchem.8b01823.

Detailed synthetic procedures and NMR spectra data, procedure of the modeling study, mass spectra data of the adduct of compound **5** and JAK3 kinase domain, kinase panel profiling data, kinetic study data of compound **32** and JAK3, and cellular activity data of compounds **3** and **5** (PDF)

Molecular formula strings and associated data (ZIP)

## ■ AUTHOR INFORMATION

### Corresponding Author

\*E-mail: [panzy@pkusz.edu.cn](mailto:panzy@pkusz.edu.cn). Phone: 86-755-26033072.

### ORCID

Yiqing Zhou: 0000-0002-6391-3259

Zhengying Pan: 0000-0002-4312-7103

### Notes

The authors declare no competing financial interest.

## ■ ACKNOWLEDGMENTS

We thank the funding support from Shenzhen Science and Technology Innovation Commission (JCYJ20160226105227446), 973 Program (2013CB910704), and the Shenzhen Municipal Development and Reform Commission.

## ■ ABBREVIATIONS

Ala, alanine; ATP, adenosine triphosphate; AUC, area under the curve; Boc, *t*-butyloxy carbonyl; BTK, Bruton's tyrosine kinase; CDI, 1,1'-carbonyldiimidazole; Cys, cysteine; DCM, dichloromethane; DIEA, diisopropylethylamine; DMF, dimethyl formamide; DMSO, dimethyl sulfoxide; EGFR, epidermal growth factor receptor; GSK3 $\beta$ , glycogen synthase kinase 3- $\beta$ ; HTRF, homogeneous time-resolved fluorescence; IL-2, interleukin-2; IL-6, interleukin-6; IL-15, interleukin-15; IFN- $\alpha$ , interferon- $\alpha$ ; ITK, interlukin-2-inducible T cell kinase; JAK, janus kinase; JAK3, janus kinase 3; Leu, leucine; LPS, lipopolysaccharide; Lys, lysine; MCP-1, monocyte chemotactic protein 1; Met, methionine; PBMC, peripheral blood mononuclear cell; PBS, phosphate-buffered saline; PE, petroleum ether; PK, pharmacokinetics; PKC, protein kinase C; RA, rheumatoid arthritis; rt, room temperature; STAT, signal transducer and activator of transcription; TFA, trifluoroacetic acid; THF, tetrahydrofuran; Val, valine

## ■ REFERENCES

- (1) Clark, J. D.; Flanagan, M. E.; Telliez, J.-B. Discovery and development of Janus kinase (JAK) inhibitors for inflammatory diseases. *J. Med. Chem.* **2014**, *57*, 5028–5038.
- (2) O'Shea, J. J.; Pesu, M.; Borie, D. C.; Changelian, P. S. A New modality for immunosuppression: targeting the JAK/STAT pathway. *Nat. Rev. Drug Discov.* **2004**, *3*, 555–564.
- (3) Flanagan, M. E.; Blumenkopf, T. A.; Brissette, W. H.; Brown, M. F.; Casavant, J. M.; Shang-Poa, C.; Doty, J. L.; Elliott, E. A.; Fisher, M. B.; Hines, M.; Kent, C.; Kudlacz, E. M.; Lillie, B. M.; Magnuson, K. S.; McCurdy, S. P.; Munchhof, M. J.; Perry, B. D.; Sawyer, P. S.; Strelevitz, T. J.; Subramanyam, C.; Sun, J.; Whipple, D. A.; Changelian, P. S. Discovery of CP-690,550: A potent and selective Janus kinase (JAK) inhibitor for the treatment of autoimmune

diseases and organ transplant rejection. *J. Med. Chem.* **2010**, *53*, 8468–8484.

(4) Thoma, G.; Nuninger, F.; Falchetto, R.; Hermes, E.; Tavares, G. A.; Vangrevelinghe, E.; Zerwes, H.-G. Identification of a potent Janus kinase 3 inhibitor with high selectivity within the Janus kinase family. *J. Med. Chem.* **2011**, *54*, 284–288.

(5) Thorarensen, A.; Dowty, M. E.; Banker, M. E.; Juba, B.; Jussif, J.; Lin, T.; Vincent, F.; Czerwinski, R. M.; Casimiro-Garcia, A.; Unwalla, R.; Trujillo, J. I.; Liang, S.; Balbo, P.; Che, Y.; Gilbert, A. M.; Brown, M. F.; Hayward, M.; Montgomery, J.; Leung, L.; Yang, X.; Soucy, S.; Hegen, M.; Coe, J.; Langille, J.; Vajdos, F.; Chrencik, J.; Telliez, J.-B. Design of a Janus Kinase 3 (JAK3) Specific inhibitor 1-((2S,5R)-5-((7H-pyrrolo[2,3-D]pyrimidin-4-yl)amino)-2-methylpiperidin-1-yl)-prop-2-en-1-one (PF-06651600) allowing for the interrogation of JAK3 signaling in humans. *J. Med. Chem.* **2017**, *60*, 1971–1993.

(6) Goedken, E. R.; Argiriadi, M. A.; Banach, D. L.; Fiamengo, B. A.; Foley, S. E.; Frank, K. E.; George, J. S.; Harris, C. M.; Hobson, A. D.; Ihle, D. C.; Marcotte, D.; Merta, P. J.; Michalak, M. E.; Murdock, S. E.; Tomlinson, M. J.; Voss, J. W. Tricyclic covalent inhibitors selectively target JAK3 through an active site thiol. *J. Biol. Chem.* **2015**, *290*, 4573–4589.

(7) Tan, L.; Akahane, K.; McNally, R.; Reyskens, K. M. S. E.; Ficarro, S. B.; Liu, S.; Herter-Sprie, G. S.; Koyama, S.; Pattison, M. J.; Labella, K.; Johannessen, L.; Akbay, E. A.; Wong, K.-K.; Frank, D. A.; Marto, J. A.; Look, T. A.; Arthur, J. S. C.; Eck, M. J.; Gray, N. S. Development of selective covalent Janus kinase 3 inhibitors. *J. Med. Chem.* **2015**, *58*, 6589–6606.

(8) Smith, G. A.; Uchida, K.; Weiss, A.; Taunton, J. Essential biphasic role for JAK3 catalytic activity in IL-2 receptor signaling. *Nat. Chem. Biol.* **2016**, *12*, 373–379.

(9) Kempson, J.; O valle, D.; Guo, J.; Wroblewski, S. T.; Lin, S.; Spengel, S. H.; Duan, J. J.-W.; Jiang, B.; Lu, Z.; Das, J.; Yang, B. V.; Hynes, J., Jr; Wu, H.; Tokarski, J.; Sack, J. S.; Khan, J.; Schieven, G.; Blatt, Y.; Chaudhry, C.; Salter-Cid, L. M.; Fura, A.; Barrish, J. C.; Carter, P. H.; Pitts, W. J. Discovery of highly potent, selective, covalent inhibitors of JAK3. *Bioorg. Med. Chem. Lett.* **2017**, *27*, 4622–4625.

(10) Elwood, F.; Witter, D. J.; Piesvaux, J.; Kraybill, B.; Bays, N.; Alpert, C.; Goldenblatt, P.; Qu, Y.; Ivanovska, I.; Lee, H.-H.; Chiu, C.-S.; Tang, H.; Scott, M. E.; Deshmukh, S. V.; Zielstorff, M.; Byford, A.; Chakravarthy, K.; Dorosh, L.; Rivkin, A.; Klappenbach, J.; Pan, B.-S.; Kariv, I.; Dinsmore, C.; Slipetz, D.; Dandliker, P. J. Evaluation of JAK3 biology in autoimmune disease using a highly selective, irreversible JAK3 inhibitor. *J. Pharmacol. Exp. Ther.* **2017**, *361*, 229–244.

(11) He, L.; Pei, H.; Lan, T.; Tang, M.; Zhang, C.; Chen, L. Design and synthesis of a highly selective JAK3 inhibitor for the treatment of rheumatoid arthritis. *Arch. Pharm.* **2017**, *350*, 1700194.

(12) Forster, M.; Chaikuad, A.; Bauer, S. M.; Holstein, J.; Robers, M. B.; Corona, C. R.; Gehringer, M.; Pfaffenrot, E.; Ghoreschi, K.; Knapp, S.; Laufer, S. A. Selective JAK3 inhibitors with a covalent reversible binding mode targeting a new induced fit binding pocket. *Cell Chem. Biol.* **2016**, *23*, 1335–1340.

(13) Thoma, G.; Drückes, P.; Zerwes, H.-G. Selective inhibitors of the Janus kinase JAK3—are they effective? *Bioorg. Med. Chem. Lett.* **2014**, *24*, 4617–4621.

(14) Thorarensen, A.; Banker, M. E.; Fensome, A.; Telliez, J.-B.; Juba, B.; Vincent, F.; Czerwinski, R. M.; Casimiro-Garcia, A. ATP-mediated kinome selectivity: the missing link in understanding the contribution of individual JAK kinase isoforms to cellular signaling. *ACS Chem. Biol.* **2014**, *9*, 1552–1558.

(15) Knight, Z. A.; Shokat, K. M. Features of selective kinase inhibitors. *Chem. Biol.* **2005**, *12*, 621–637.

(16) Swinney, D. C. Biochemical mechanisms of drug action: what does it take for success? *Nat. Rev. Drug Discov.* **2004**, *3*, 801–808.

(17) Cheng, H.; Nair, S. K.; Murray, B. W.; Almaden, C.; Bailey, S.; Baxi, S.; Behenna, D.; Cho-Schultz, S.; Dalvie, D.; Dinh, D. M.; Edwards, M. P.; Feng, J. L.; Ferre, R. A.; Gajiwala, K. S.; Hemkens, M. D.; Jackson-Fisher, A.; Jalaie, M.; Johnson, T. O.; Kania, R. S.;

Kephart, S.; Lafontaine, J.; Lunney, B.; Liu, K. K.-C.; Liu, Z.; Matthews, J.; Nagata, A.; Niessen, S.; Ornelas, M. A.; Orr, S. T. M.; Pairish, M.; Planken, S.; Ren, S.; Richter, D.; Ryan, K.; Sach, N.; Shen, H.; Smeal, T.; Solowiej, J.; Sutton, S.; Tran, K.; Tseng, E.; Vernier, W.; Walls, M.; Wang, S.; Weinrich, S. L.; Xin, S.; Xu, H.; Yin, M.-J.; Zientek, M.; Zhou, R.; Kath, J. C. Discovery of 1-((3R,4R)-3-[(5-chloro-2-[(1-methyl-1H-pyrazol-4-yl)amino]-7H-pyrrolo[2,3-D]-pyrimidin-4-yl)oxy)methyl]-4-methoxypyrrolidin-1-yl)prop-2-en-1-one (PF-06459988), a potent, WT sparing, irreversible inhibitor of T790M-containing EGFR mutants. *J. Med. Chem.* **2016**, *59*, 2005–2024.

(18) Telliez, J.-B.; Dowty, M. E.; Wang, L.; Jussif, J.; Lin, T.; Li, L.; Moy, E.; Balbo, P.; Li, W.; Zhao, Y.; Crouse, K.; Dickinson, C.; Symanowicz, P.; Hegen, M.; Banker, M. E.; Vincent, F.; Unwalla, R.; Liang, S.; Gilbert, A. M.; Brown, M. F.; Hayward, M.; Montgomery, J.; Yang, X.; Bauman, J.; Trujillo, J. I.; Casimiro-Garcia, A.; Vajdos, F. F.; Leung, L.; Geoghegan, K. F.; Quazi, A.; Xuan, D.; Jones, L.; Hett, E.; Wright, K.; Clark, J. D.; Thorarensen, A. Discovery of a JAK3-selective inhibitor: functional differentiation of JAK3-selective inhibition over pan-JAK or JAK1-selective inhibition. *ACS Chem. Biol.* **2016**, *11*, 3442–3451.

(19) Pattison, M. J.; MacKenzie, K. F.; Arthur, J. S. C. Inhibition of JAKs in macrophages increases lipopolysaccharide-induced cytokine production by blocking IL-10-mediated feedback. *J. Immunol.* **2012**, *189*, 2784–2792.

(20) Bisswanger, H. *Enzyme Kinetics: Principles and Methods*; Wiley-VCH: Weinheim, 2002; pp 103–106.